Heliyon 10 (2024) e28882

Contents lists available at ScienceDirect

Heliyon

journal homepage: www.cell.com/heliyon

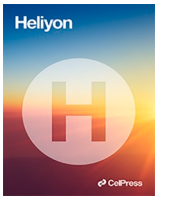

Research article

LncRNA MALAT1 suppresses monocyte-endothelial cell interactions by targeting miR-30b-5p and enhancing ATG5-mediated autophagy

Xiaodong Gu [a,b,d,1], Jingyuan Hou [a,b,d,1], Jiawei Rao [c], Ruiqiang Weng [a,b,d], Sudong Liu [a,b,d,*]

[a] Meizhou Clinical Institute, Shantou University Medical College, Meizhou, 514000, China
[b] Research Experimental Center, Meizhou People's Hospital (Huangtang Hospital), Meizhou, 514031, China
[c] Meizhou Clinical Medical School, Guangdong Medical University, Meizhou, 514000, China
[d] Guangdong Engineering Technology Research Center of Molecular Diagnostics for Cardiovascular Diseases, Meizhou, 514000, China

ARTICLE INFO

Keywords:
Long non-coding RNA
Metastasis associated lung adenocarcinoma transcript 1
Inflammation
Monocyte-endothelial cell interaction
Atherosclerosis
Autophagy

ABSTRACT

Background: Monocyte-endothelial cell (EC) interactions are one of the earliest events in the development of atherosclerosis and play a crucial role in atherosclerotic plaque formation. Although attempts have been made to modulate this interaction, the underlying molecular signalling mechanisms remain unclear. This study aimed to investigate the role of long non-coding RNA MALAT1 in monocyte-EC interactions.

Methods: The expression of MALAT1, ICAM-1, VCAM-1, P-selectin, CCL2 and CXCL1 was evaluated in ApoE$^{-/-}$ mouse aortic tissues and inflamed human umbilical vein endothelial cells (HUVECs). The regulatory impact of MALAT1 on cell adhesion molecules, monocyte-EC adhesion, and autophagy was assessed. The interactions between MALAT1 and microRNAs (miRNAs) were evaluated using dual-luciferase reporter and RNA pull-down assays.

Results: MALAT1 expression decreased in ApoE$^{-/-}$ mouse aortic tissues and inflammatory HUVECs. MALAT1 overexpression suppressed the expression of ICAM-1, VCAM-1 and CXCL1, and reduced the migration and adhesion of monocytes to ECs. Inhibition of MALAT1 promoted cell adhesion molecule expression and monocyte-EC interactions. Mechanistically, MALAT1 binds directly to miR-30b-5p and decreases its effective expression by functioning as an endogenous sponge, thereby increasing the expression of autophagy-related gene 5 (ATG5) and stimulates endothelial autophagy.

Conclusions: Our findings suggest that MALAT1 suppresses monocyte-EC interactions by targeting miR-30b-5p and enhancing ATG5-mediated endothelial autophagy. These data imply that MALAT1 may play a protective role at the early stages of the atherosclerotic process.

1. Introduction

Cardiovascular disease (CVD) is a major cause of morbidity and mortality worldwide [1]. Atherosclerosis is the most common cause

* Corresponding author. Meizhou People's Hospital (Huangtang Hospital), Meizhou, 514031, China.
E-mail address: vanguard_1987@163.com (S. Liu).
[1] These authors contributed equally to this work.

https://doi.org/10.1016/j.heliyon.2024.e28882
Received 27 September 2023; Received in revised form 26 March 2024; Accepted 26 March 2024
Available online 3 April 2024

of CVD. The development of atherosclerotic plaques is a complex process comprised of multiple events that are triggered by endothelial activation, followed by monocyte recruitment and foam cell formation [2]. Thus, modulation of monocyte-endothelial interactions represents a viable strategy for preventing the development of atherosclerosis at an early stage. However, the mechanisms underlying the regulation of this process are not fully understood.

The adhesion of circulating monocytes to endothelial cells (ECs) is mediated by various cell adhesion molecules (CAMs) expressed on the surface of ECs and monocytes, including selectins, intercellular adhesion molecule-1 (ICAM-1), vascular cell adhesion molecule 1(VCAM-1), and integrins [3]. CAMs are known inflammatory biomarkers of atherosclerosis and are involved in leukocyte recruitment, endothelial dysfunction, and thrombosis. Evidence indicates that elevated CAM expression or activity in response to various stimuli, such as inflammation, hyperlipidaemia, and oxidative stress, significantly enhances leukocyte recruitment and promotes atherogenesis [4]. Additionally, elevated soluble CAM levels are associated with increased severity of atherosclerosis [5]. Previous studies have found that ICAM-1, VCAM-1 and P-selectin play essential roles in regulating the rolling velocity and adhesion of leukocytes to facilitate their paracellular or transcellular migration [6]. Thus, CAMs are attractive therapeutic targets for the treatment of atherosclerosis.

Long noncoding RNAs (lncRNAs) are a class of noncoding RNAs with a >200 nucleotide length that do not encode proteins [7]. Accumulating evidence suggests that lncRNAs act as crucial regulators of gene expression and other biological processes [7]. Mechanistically, lncRNAs can interact directly with DNA or proteins to exert their effects, or act as a sponge for miRNAs to competitively interfere with miRNA functions [8,9]. Although most early lncRNAs were discovered in cancers, an increasing number of them have been identified in CVDs [10]. Myocardial infarction-associated transcript (MIAT) is one of the earliest lncRNAs discovered in acute myocardial infarction (AMI) and plays a regulatory role in atherosclerotic lesion formation and plaque destabilisation [11]. LncRNA ANRIL (antisense non-coding RNA in the INK4 locus) promotes the development of atherosclerosis, and lncRNA MHRT (myosin heavy-chain-associated RNA transcripts) protects the heart from pathological hypertrophy [12,13]. LncRNA MALAT1 (metastasis-associated lung adenocarcinoma transcript 1), first identified in lung adenocarcinoma, is a tumour-associated lncRNA involved in a wide range of biological and cellular processes [14]. Later studies have found that MALAT1 plays a crucial role in endothelial and smooth muscle cell proliferation [15,16]. Reduced levels of MALAT1 were found to augment atherosclerotic lesion formation in mice. Bone marrow cells isolated from MALAT1$^{-/-}$ mice showed an increased adhesion to ECs and elevated levels of proinflammatory mediators [17].

The aim of this study was to explore the role of MALAT1 in monocyte-EC interactions as well as the development of endothelial dysfunction and atherosclerosis. The findings of our study suggest that lncRNA MALAT1 suppresses monocyte migration and adhesion to ECs by reducing CAM expression, highlighting a protective role of this lncRNA in atherosclerosis progression.

2. Materials and methods

2.1. Mice

All animal experiments were approved by the Laboratory Animal Ethics Committee of Guangdong Medical University (Ethical Approval Number: GDY2002177) and were performed in accordance with the National Guidelines for Animal Care and Use. Male ApoE$^{-/-}$ C57BL/6 mice (6–8 weeks of age) were obtained from Changzhou CAVENS Laboratory Animal Co., Ltd. (Changzhou, China). To establish an atherosclerosis model, the mice were fed a high-fat diet (D12108C, New Brunswick, NJ, USA) containing 20% fat and 1.25% cholesterol for 12 weeks. As controls, male ApoE$^{-/-}$ C57BL/6 mice were fed a normal chow diet for 12 weeks. Mice were anaesthetised with sodium pentobarbital and euthanised. Aortas were excised, fixed in 4% paraformaldehyde, pinned, and stained with oil red O (Beyotime, Shanghai, China) to detect lipid deposition. All aortic tissues were stored in liquid nitrogen until use.

2.2. Cell culture

Primary human umbilical vein ECs (HUVECs) were purchased from the BeNa Culture Collection (BNCC342438; Beijing, China). HUVECs were cultured in endothelial cell basal medium (Sciencell, CA, USA) supplemented with endothelial cell growth supplement (ECGS; Sciencell, CA, USA) and 5% foetal bovine serum (FBS; Sciencell, CA, USA) until the third passage. The human monocyte cell line (THP-1) was cultured in RPMI-1640 medium containing 10% FBS (Gibco, Carlsbad, CA, USA). Human embryonic kidney cells (HEK293T) were cultured in DMEM supplemented with 10% FBS (Gibco). Cells were cultured at 37 °C in a humidified atmosphere containing 5% CO_2.

2.3. Cell transfection

To achieve MALAT1 overexpression, the full-length MALAT1 sequence (NR_002819.4) was synthesised by GenePharma (Shanghai, China), and inserted into the pcDNA3.1-EGFP vector (pcDNA3.1-MALAT1) to construct a MALAT1 overexpression vector. HUVECs were seeded at 2.0×10^5 cells per well in 12-well plates and incubated overnight, followed by transfection with 100 ng of pcDNA 3.1-MALAT1 or pcDNA 3.1-NC (negative control) using Lipofectamine™ 3000 (Invitrogen, CA, USA). To knock down MALAT1, anti-sense oligo (ASO)-MALAT1 (AGGTGCTACACAGAAGTGGA) and ASO-negative control (NC) reagents were purchased from RiboBio (Guangzhou, China) and transfected into HUVECs at a concentration of 25 nM using Lipofectamine™ 3000.

MiR-30b-5p mimic (5′-3': TGTAAACATCCTACACTCAGCT, 3′-5': ACATTTGTAGGATGTGAGTCGA) and control mimic were purchased from RiboBio (Guangzhou, China) and transfected into HUVECs at a concentration of 25 nM using Lipofectamine™ 3000. Small

interfering RNAs (siRNAs) (TGACGTTGGTAACTGACAA; RiboBio) targeting the autophagy-related gene 5 (ATG5) were transfected into HUVECs at a concentration of 25 nM siRNA-ATG5 or siRNA-negative control using Lipofectamine™ 3000.

2.4. Enzyme-linked immunosorbent assay (ELISA)

The production of ICAM-1, VCAM-1, P-selectin, CCL2, and CXCL1 in the culture supernatant was detected using Human ELISA kits (Multisciences, Hangzhou, China), according to the manufacturer's instructioins. Optical density was measured using a Varioskan Flash ELISA reader (Thermo Fisher Scientific, Waltham, MA, USA).

2.5. RNA isolation and quantitative reverse transcription-polymerase chain reaction (qRT-PCR)

Total RNA was isolated from mouse aortic tissues or cells using the TRIzol reagent (Invitrogen, Carlsbad, CA, USA). RNA quality was determined based on the A260/A280 ratio using an ultramicro-spectrophotometer (NP80, IMPLEN, Germany). A Takara reverse transcription kit (either the Prime Script RT reagent kit or Mir-X™ miRNA first-strand synthesis kit; Takara Bio, Tokyo, Japan) was used to generate complementary DNA (cDNA). The cDNA template was amplified by qRT-PCR using the TB Green™ Premix Ex Taq™ II kit or the TB Green™ qRT-PCR kit (Takara Bio, Tokyo, Japan). The expression of messenger RNA (mRNA) was normalised to GAPDH while the expression of miRNA was normalised to U6 RNA using the $2^{-\Delta\Delta Ct}$ relative quantification method. The primers used in these assays are listed in Table 1.

2.6. Cell adhesion assay

The monocyte-EC adhesion assay was conducted as previously described [18]. Briefly, THP-1 cells were placed in serum-free RPMI-1640 medium and labeled with carboxifluorescein diacetate succinimidyl ester (CFSE; Molecular Probes, Leiden, Netherlands) at a concentration of 5 μM and incubated at 37 °C for 10 min. RPMI-1640 medium containing 20% FBS was added to stop the labelling reaction. THP-1 cells were centrifuged, washed twice with phosphate-buffered saline (PBS), and added to a confluent HUVECs monolayer. After 1 h, the non-adherent THP-1 cells were gently washed off with PBS. The adhesion between THP-1 cells and HUVECs was observed and photographed using fluorescence microscopy (DMi8; Leica, Wetzlar, Germany). Image-Pro Plus software (version 6.0) was used for statistical analysis of the acquired fluorescent micrographs.

Table 1
Primers sequence for qRT-PCR.

Gene	Forward (5′-3′)	Reverse (5′-3′)
Ms MALAT1	CATGGCGGAATTGCTGGTA	TGCCAACAGCATAGCAGTA
Ms ICAM-1	GTGATGCTCAGGTATCCATCCA	CACAGTTCTCAAAGCACAGCG
Ms VCAM-1	TTGGGAGCCTCAACGGTACT	GCAATCGTTTTGTATTCAGGGGA
Ms P-selectin	TCGGATCCCTTCGGTACCTT	ACAGCTTGACATTCGGGAGG
Ms CCL2	TAAAAACCTGGATCGGAACCAAA	GCATTAGCTTCAGATTTACGGGT
Ms CXCL1	ACTGCACCCAAACCGAAGTC	TGGGGACACCTTTTAGCATCTT
Ms GAPDH	AGGTCGGTGTGAACGGATTTG	TGTAGACCATGTAGTTGAGGTCA
Hu MALAT1	GTGATGCGAGTTGTTCTCCG	CTGGCTGCCTCAATGCCTAC
Hu ICAM-1	CTCCAATGTGCCAGGCTTG	CAGTGGGAAAGTGCCATCCT
Hu VCAM-1	GGACCACATCTACGCTGACA	TTGACTGTGATCGGCTTCCC
Hu P-selectin	ATGGGTGGGAACCAAAAAGG	GGCTGACGGACTCTTGATGTAT
Hu CCL2	CAGCCAGATGCAATCAATGCC	TGGAATCCTGAACCCACTTCT
Hu CXCL1	CTGGCGGATCCAAGCAAATG	GCCCCTTTGTTCTAAGCCAG
Hu ATG1A	GGCAAGTTCGAGTTCTCCCG	CGACCTCCAAATCGTGCTTCT
Hu ATG2A	GAGATCGCCGGCCAGAAG	AGGTCACGCTGGTTGATGAG
Hu ATG3	GACCCCGGTCCTCAAGGAA	TGTAGCCCATTGCCATGTTGG
Hu ATG4A	TTCTTGGACCCTCATACAACCC	TTAGGATGTTCATTCGCTGTGG
Hu ATG5	AAAGATGTGCTTCGAGATGTGT	CACTTTGTCAGTTACCAACGTCA
Hu ATG7	CAGTTTGCCCCTTTTAGTAGTGC	CCAGCCGATACTCGTTCAGC
Hu ATG10	ATAAGATGCGACTGCTACAGGG	CAATGCTCAGCCATGATGTGAT
Hu ATG12	CTGCTGGCGACACCAAGAAA	CGTGTTCGCTCTACTGCCC
Hu ATG13	TTGCTATAACTAGGGTGACACCA	CCCAACACGAACTGTCTGGA
Hu ATG16L	CTGCTGGCGACACCAAGAAA	CGTGTTCGCTCTACTGCCC
Hu GAPDH	ATGACATCAAGAAGGTGGTG	CATACCAGGAAATGAGCTTG
miR-30b-5p	TGTAAACATCCTACACTCAGCT	*
miR-216b-5p	AAATCTCTGCAGGCAAATGTGA	*
miR-99a-3p	CAAGCTCGCTTCTATGGGTCTG	*
U6	GGAACGATACAGAGAAGATTAGC	TGGAACGCTTCACGAATTTGCG

Ms: Mus musculus; Hu: Homo sapiens.
*The downstream universal primer sequence from TB Green™ RT-qPCR kit was not provided.

2.7. Migration assay

HUVECs were harvested after different treatments and centrifuged. The supernatant (representing cell-free conditioned medium) was collected and dispensed into a 24-well plate in 600 μl aliquots per well. A transwell chamber apparatus (24-well plates; 8-μm pore size), was employed for the migration assay according to the manufacturer's instructions (Costar/Corning Incorporated, USA). Aliquots of 2.5×10^5 THP-1 cells in RPMI-1640 medium were seeded into a transwell chamber. After incubation for 24 h, the migration chamber was removed, and THP-1 cells present in the 24-well plate wells were collected and counted.

2.8. Luciferase reporter assay

Truncated MALAT1 sequences containing the predicted miR-30b-5p binding site (TGTTTAC) or a mutated sequence (ACAAATG) were chemically synthesised and purchased from GenePharma (Shanghai, China), and inserted into the psiCHECK-2 luciferase reporter vector (psiCHECK-2-MALAT1-wt and psiCHECK-2-MALAT1-mut, respectively). HEK293T cells were seeded in 24-well plates with 2.0×10^4 cells per well and incubated overnight. Then, psiCHECK-2-MALAT1-wt or psiCHECK-2-MALAT1-mut and either the miR-30b-5p mimic or control mimic were co-transfected into the cells using Lipofectamine™ 3000. After 48 h, relative luciferase activity was detected using the Dual-Glo Luciferase Assay System (Promega, Madison, WI, USA) according to the manufacturer's instructions. Luciferase activity was measured and normalised to Renilla luminescence.

2.9. RNA pull-down assay

The interaction between MALAT1 and miRNAs in ECs was validated using an RNA pull-down assay. Biotinylated DNA probes complementary to MALAT1 and antisense RNA (control) were purchased from GenePharma (Shanghai, China). MALAT1-binding RNA was captured using a Pierce™ RNA Magnetic RNA-protein Pull-Down Kit (Thermo Scientific, Rockford, IL, USA). Briefly, cell lysates were prepared and incubated with biotinylated probe and streptavidin magnetic beads (Sigma-Aldrich, St. Louis, MO). Total RNA was extracted from the pull-down samples, and miR-30b-5p levels were analyzed by qRT-PCR.

2.10. Western blotting

The cells were lysed in RIPA lysis buffer (Beyotime Biotechnology, Shanghai, China) containing protease and phosphatase inhibitors. The protein concentration was determined using a bicinchoninic acid kit (Abcam, Cambridge, MA, USA). Protein samples were run on 4–20% gradient gels and transferred onto a PVDF membrane. After blocking with 5% nonfat milk in Tris-buffered saline with 0.05% Tween-20 (TBST), the membranes were incubated with the primary antibody (Ab). After washing, the membranes were incubated with HRP peroxidase-conjugated secondary anti-rabbit or anti-mouse antibodies (Abcam). The bands were visualised using chemiluminescence (ECL; Meilunbio, Dalian, China). The results were imaged using the ChemiDoc MP ultrasensitive imaging system (Bio-Rad, Hercules, CA, USA). The proteins were quantified by analysing the band intensity of the Western blot images via ImageJ software (NIH, Bethesda, MD, USA). Primary Abs used in the present study included: ICAM-1 (1:2000; Abcam, MA, USA), VCAM-1 (1:5000; Abcam), p-IκBα (1:2000; Cell Signalling Technology, MA, USA), NF-κB p65 (1:2000; Abcam), p-NF-κB p65 (1:2000; Cell Signalling Technology), ATG5 (1:2000; Cell Signalling Technology), ATG13 (1:2000; Cell Signalling Technology), SQSTM1 (1:2000; Cell Signalling Technology), LC3B (1:2000; Cell Signalling Technology) and GAPDH (1:5000; Sigma, MO, USA).

2.11. Immunofluorescence staining assay

Immunofluorescence staining assay was used for the detection of NF-κB p65 nuclear translocation and LC3B transformation. HUVECs were transfected with pcDNA 3.1-MALAT1 and stimulated with TNF-α (10 ng/mL) in the presence or absence of bafilomycin for 24 h. HUVECs were fixed with 4% paraformaldehyde for 1 h and permeabilised with 0.5% Triton X-100 for 30 min, and subsequently blocked with bovine serum albumin for 1 h. HUVECs were incubated with anti-NF-κB p65 antibody (Beyotime) at 4 °C overnight. After gentle washing, anti-rabbit Cy3 Ab was added to the fixed and permeabilised cell monolayers and incubated at 37 °C for 1 h. The reaction was stopped using 4',6-diamidino-2-phenylindole. The cells were then visualised and images were captured using a confocal microscope (LSM 900, Zeiss, Germany).

To detect autophagy, immunofluorescence staining of LC3B-positive autophagosomes was carried out using an LC3B antibody kit for autophagy (Cell Signalling Technology). The staining was performed according to the manufacturer's instructions. The number of endogenous LC3B puncta was evaluated by confocal microscopy (LSM 900; Zeiss, Germany).

2.12. Statistical analysis

Statistical analyses were performed using the SPSS software (version 20.0; IBM Corp., Armonk, NY, USA). Continuous variables were expressed as mean ± standard deviation (SD). The Shapiro-Wilk test was applied to determine the normality of the distribution of continuous variables. Student's t-test or Mann-Whitney *U* test was used for comparisons between two groups when appropriate. A *P*-value of <0.05 was considered as statistically significant.

3. Results

3.1. Expression of MALAT1 decreases in atherosclerotic aortic tissue and inflamed ECs

To investigate the role of MALAT1 in atherosclerosis (AS), we established a mouse model of AS (Fig. 1A). MALAT1 expression was significantly decreased in the aortas of atherosclerotic (AS) mice compared to control mice (Fig. 1B). We examined the expression of inflammatory mediators, including ICAM-1, VCAM-1, P-selectin, CCL2, and CXCL1, and found that these genes were profoundly upregulated in AS mice compared to the controls (Fig. 1C). Furthermore, MALAT1 expression was significantly decreased in HUVECs after treatment with IL-1β, lipopolysaccharide (LPS) or TNF-α (Fig. 1D) and reflected the dose-dependent manner of TNF-α stimulation (Fig. 1E). Additionally, the expression of ICAM-1, VCAM-1, P-selectin, CCL2 and CXCL1 were significantly elevated after TNF-α stimulation (Fig. 1F). Together, these results suggest that MALAT1 may participate in the vascular EC inflammation process during atherosclerosis development.

3.2. MALAT1 inhibits the expression of cell adhesion molecules and monocyte-EC interactions

To confirm the effects of MALAT1 on cell adhesion molecules, HUVECs were transfected with pcDNA 3.1-MALAT1 or ASO-MALAT1 (Fig. 2A). The results showed that MALAT1 overexpression significantly inhibited the expression of ICAM-1, VCAM-1, and CXCL1 at both the mRNA and protein levels, whereas MALAT1 knockdown enhanced the expression of these genes (Fig. 2, B-D). During atherosclerotic lesion formation, monocytes migrate and adhere to the vessel endothelium via adhesion molecules. Therefore, we investigated the functional relevance of MALAT1 in monocyte migration and adhesion to ECs. Transwell migration assays showed that MALAT1 overexpression prevented THP-1 migration to HUVECs, whereas MALAT1 knockdown promoted this process (Fig. 2E). The adhesion assay data showed that MALAT1 overexpression significantly decreased the number of THP-1 cells bound to the HUVEC monolayer, whereas MALAT1 knockdown increased the number of adherent THP-1 cells (Fig. 2F). Taken together, these data suggest that MALAT1 suppresses the migration and adhesion of monocytes to ECs during the inflammatory response.

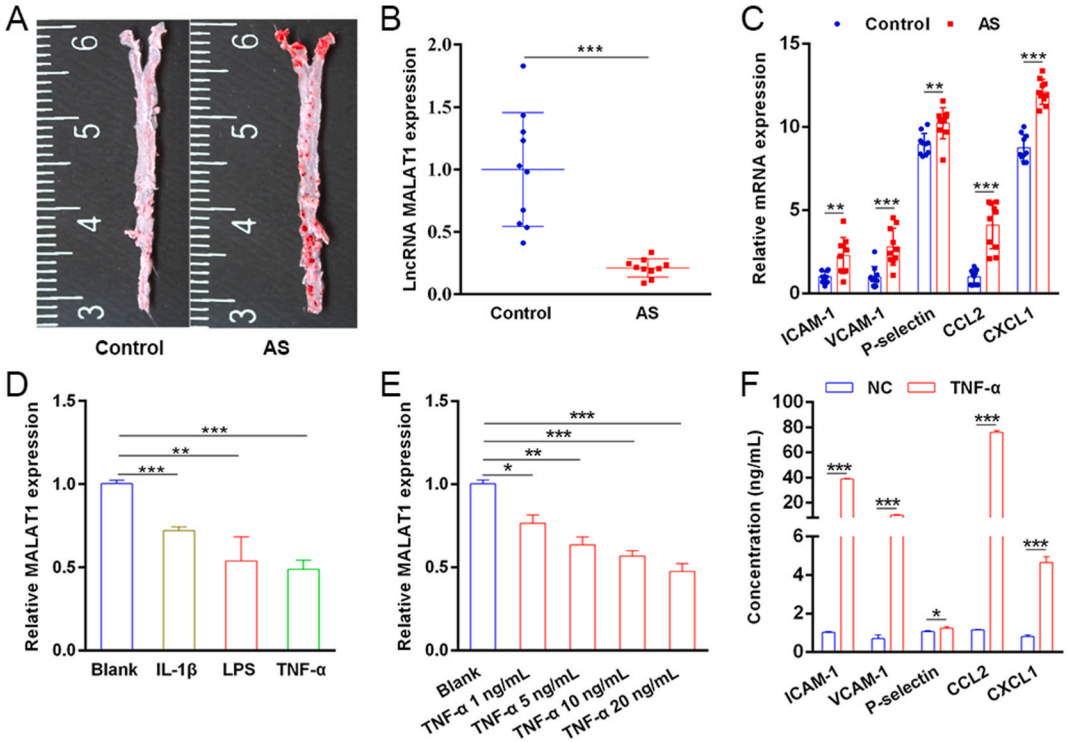

Fig. 1. Expression of MALAT1 is reduced in atherosclerotic aortic tissue and inflamed ECs. (**A**) Murine aortas were examined by oil red O staining. (**B**) The expression of MALAT1 in aortic tissues of AS mice (n = 10) and controls (n = 10) was detected by qRT-PCR. (**C**) The expression of inflammatory mediators in aortic tissue of AS mice (n = 10) and controls (n = 10) was detected by qRT-PCR. (**D**) HUVECs were stimulated with IL-1β (200 ng/mL), LPS (100 ng/mL) or TNF-α (10 ng/mL) for 24 h, and expression of MALAT1 was detected by qRT-PCR. (**E**) HUVECs were treated with TNF-α (1, 5, 10, 20 ng/mL) for 24 h, and MALAT1 levels were detected by qRT-PCR. (**F**) HUVECs were stimulated with TNF-α (10 ng/mL) and the expression of ICAM-1, VCAM-1, P-selectin, CCL2 and CXCL1 were detected by qRT-PCR. *, $P < 0.05$; **, $P < 0.01$; ***, $P < 0.001$.

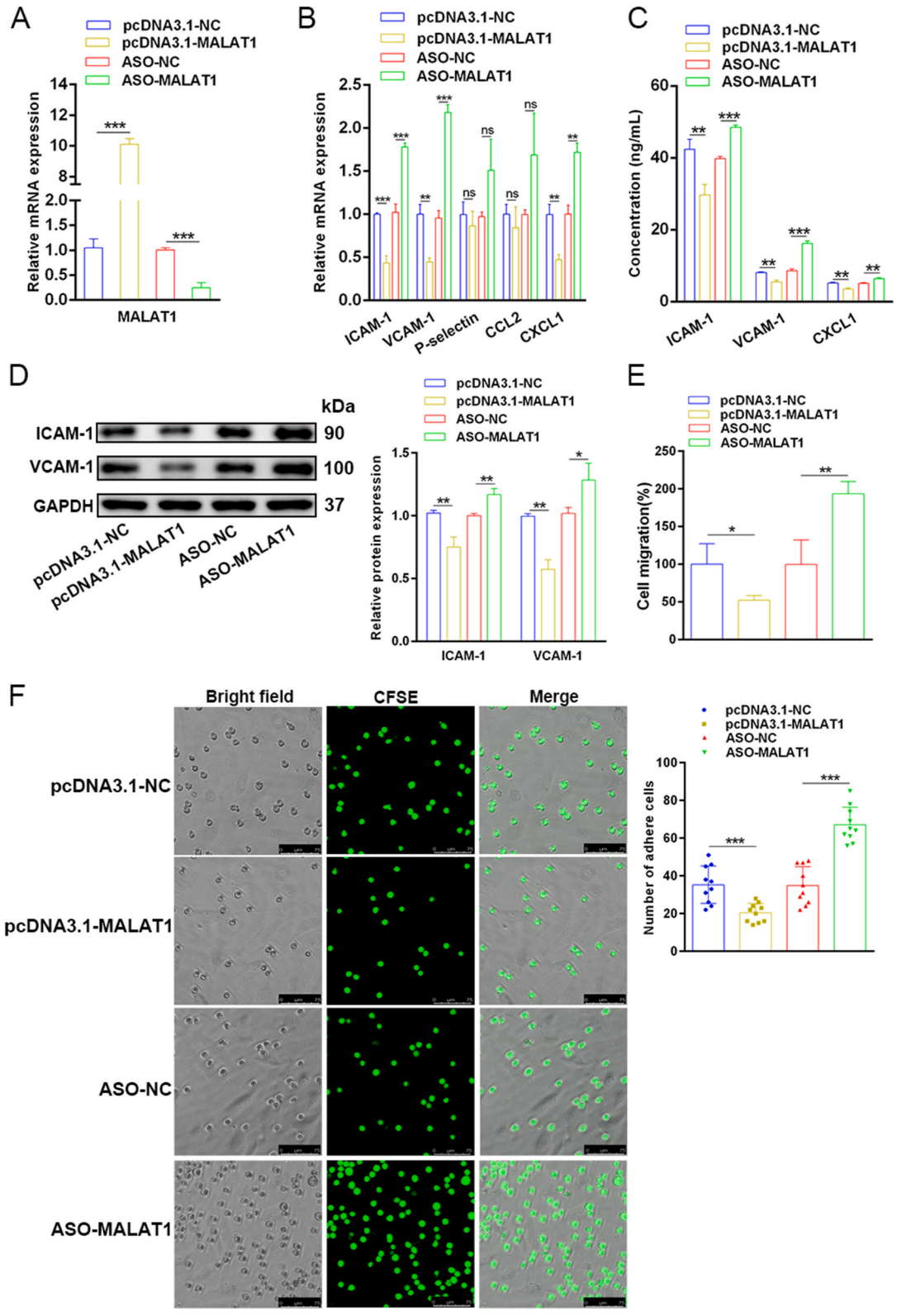

Fig. 2. MALAT1 inhibits the expression of adhesion molecules and monocyte-EC interactions (**A**) HUVECs were transfected with pcDNA3.1-MALAT1 or ASO-MALAT1, and MALAT1 levels were detected by qRT-PCR. (**B-D**) HUVECs were transfected with pcDNA3.1-MALAT1 or ASO-MALAT1, followed by TNF-α stimulation (10 ng/mL) for 24 h. The expression of inflammatory mediators was detected by qRT-PCR, ELISA, or

western blotting. (**E**) The functional impact of MALAT1 on monocyte migration was assessed by a migration assay. **(F)** The effect of MALAT1 on monocyte-EC adhesion was evaluated by a cell adhesion assay. Scale bar: 75 μm. Data are shown as mean ± SD (n = 3). *, $P < 0.05$; **, $P < 0.01$; ***, $P < 0.001$; ns, not significant.

3.3. Induction of endothelial autophagy following overexpression of MALAT1 reduces NF-κB activity

NF-κB signalling has been reported to regulate the expression of adhesion molecules. Hence, we investigated whether MALAT1 repressed NF-κB activity. HUVECs were transfected with pcDNA 3.1-MALAT1 followed by TNF-α stimulation. It was observed that MALAT1 overexpression suppressed the expression of phosphorylated (p)-NF-κB p65 and p-IκBα as detected by western blotting (Fig. 3A). Meanwhile, the nuclei of ECs overexpressing MALAT1 contained much more p65 than those of controls (Fig. 3B). Next, we

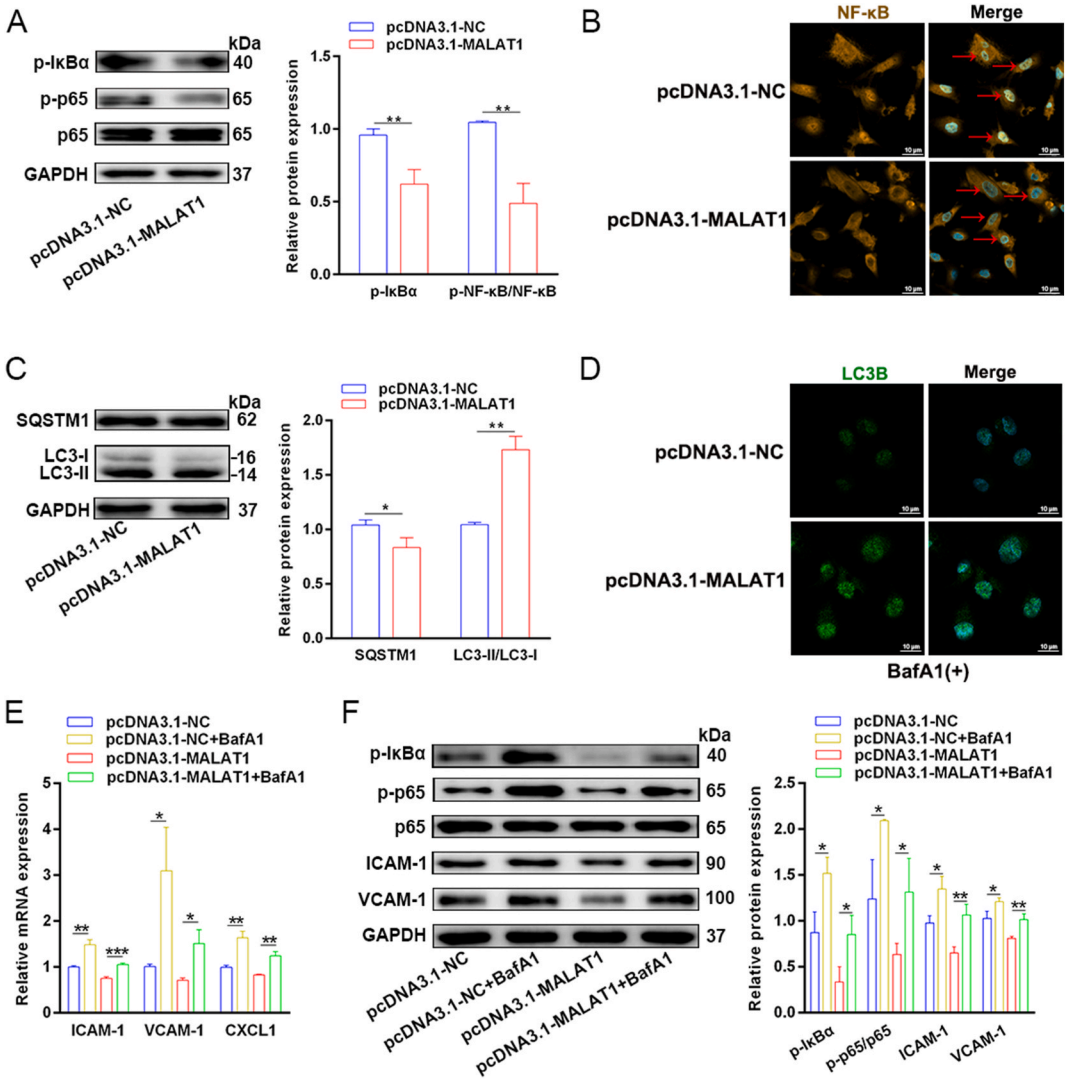

Fig. 3. Induction of endothelial autophagy following overexpression of MALAT1 reduces NF-κB activity. (**A**) HUVECs were transfected with pcDNA3.1-MALAT1 followed by TNF-α stimulation (10 ng/mL) and the protein levels of p-NF-κB p65 and p-IκBα were quantified via immunoblotting. (**B**) HUVECs were transfected with pcDNA3.1-MALAT1 followed by TNF-α (10 ng/mL) stimulation, and the nuclear transport of NF-κB p65 was detected by an immunofluorescence assay. Scale bar: 10 μm. (**C**) HUVECs were transfected with pcDNA3.1-MALAT1 followed by TNF-α stimulation (10 ng/mL) and the protein levels of LC3B (LC3II/LC3I) and SQSTM1 were quantified via immunoblotting. (**D**) HUVECs were transfected with pcDNA3.1-MALAT1 followed by treatment with TNF-α (10 ng/mL) and bafilomycin A1 (BafA1, 100 nM) for 24 h and endogenous LC3B puncta levels were analyzed by fluorescence assays. Scale bar: 10 μm. (**E**) HUVECs were transfected with pcDNA3.1-MALAT1 followed by TNF-α stimulation (10 ng/mL) and the mRNA levels of ICAM-1, VCAM-1 and CXCL1 were detected by qRT-PCR, (**F**) The protein levels of p-IκBα, p-NF-κB p65, ICAM-1 and VCAM-1 were quantified by western blotting. Data are shown as mean ± standard deviation (n = 3). *, $P < 0.05$; **, $P < 0.01$; ***, $P < 0.001$.

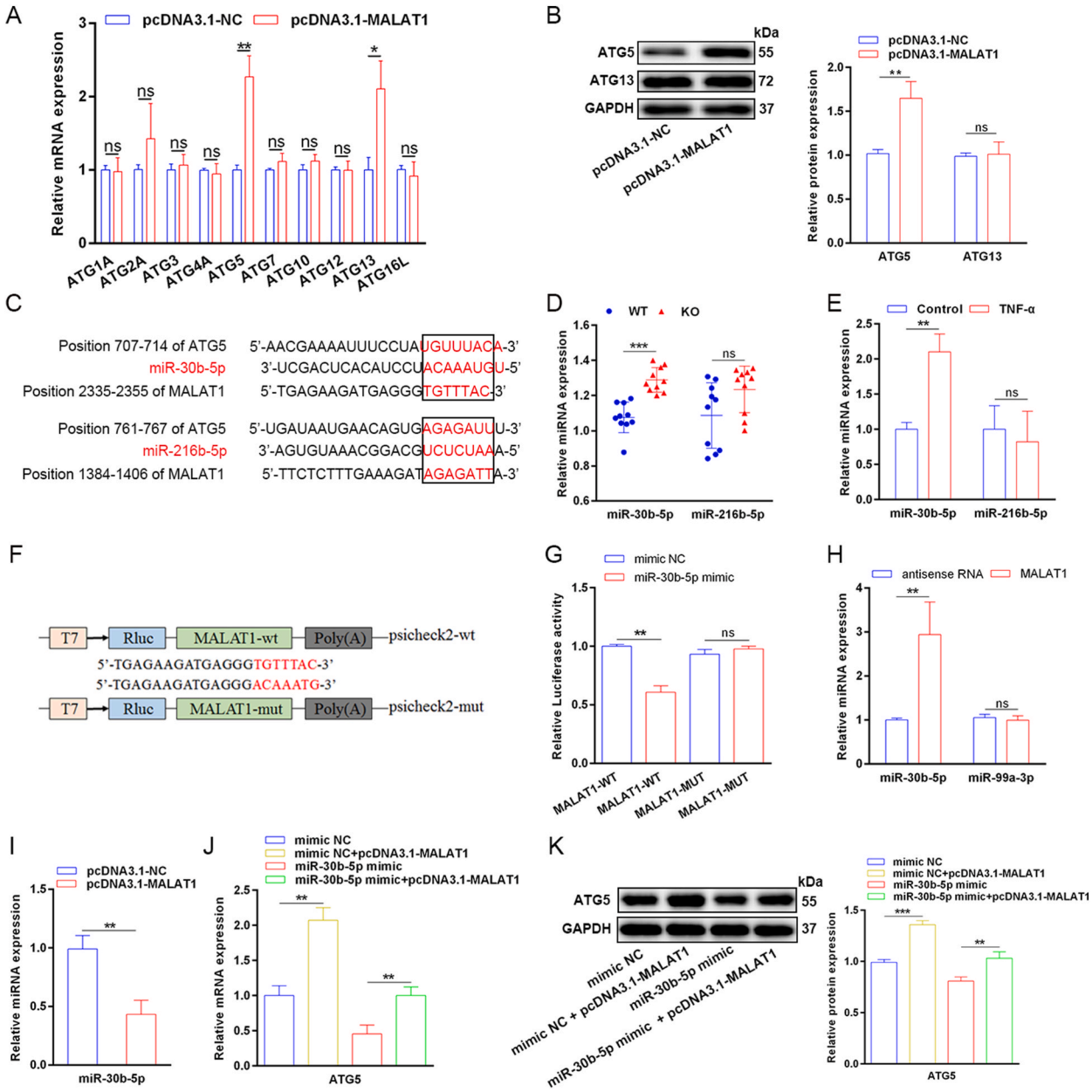

Fig. 4. MALAT1 binds to miR-30b-5p and enhances ATG5 expression. (**A**) HUVECs were transfected with pcDNA3.1-MALAT1 followed by TNF-α (10 ng/mL) treatment and qRT-PCR was used to detect the expression of ATGs. (**B**) The protein levels of ATG5 and ATG13 were quantified by western blotting. (**C**) Bioinformatics analysis of the putative binding between miR-30b-5p, miR-216b-5p, ATG5 mRNA and MALAT1 LncRNA. (**D-E**) The expression of miR-30b-5p and miR-216b-5p in aortic tissues and TNF-α-treated HUVECs was detected by qRT-PCR. (**F**) The psicheck2-based luciferase reporter plasmids containing wild-type MALAT1 (psicheck2-MALAT1-wt) and mutated MALAT1-reporter sequences (psicheck2-MALAT1-mut) are presented with the putative miR-30b-5p binding sites shown in red font. (**G**) Psicheck2-based luciferase reporter constructs and miR-30b-5p mimic were co-transfected into HEK293T cells for 48 h followed by reporter activity measurement via dual luciferase reporter assays. (**H**) HUVEC lysates were incubated with biotin-labeled MALAT1 or antisense RNA (synthesised *in vitro*) for biotin pull-down detection, and miR-30b-5p and miR-99a-3p levels were analyzed. (**I**) The expression of miR-30b-5p in HUVECs transfected with pcDNA3.1-MALAT1 followed by TNF-α stimulation was analyzed by qRT-PCR. (**J**) HUVECs were transfected with miR-30b-5p mimic and/or pcDNA3.1-MALAT1 followed by TNF-α stimulation (10 ng/mL) and ATG5 mRNA levels were detected by qRT-PCR. (**K**) Western blotting was used to measure ATG5 protein levels in inflamed HUVECs transfected with miR-30b-5p mimic and/or pcDNA3.1-MALAT1. Data are shown as mean ± standard deviation (n = 3). *, $P < 0.05$; **, $P < 0.01$; ***, $P < 0.001$; ns, not significant.

probed how MALAT1 interfered with NF-κB signalling. Previous studies have indicated that endothelial autophagy plays a crucial role in modulating NF-κB signalling. Thus, we investigated whether MALAT1 affects endothelial autophagy. Overexpression of MALAT1 significantly induced endothelial autophagy, as indicated by a decrease in SQSTM1 expression and an enhancement of the conversion of LC3I to LC3BII (Fig. 3C). Similarly, overexpression of MALAT1 led to a significant increase in LC3B-positive autophagosomes in HUVECs after bafilomycin A1 (BafA1) treatment (Fig. 3D).

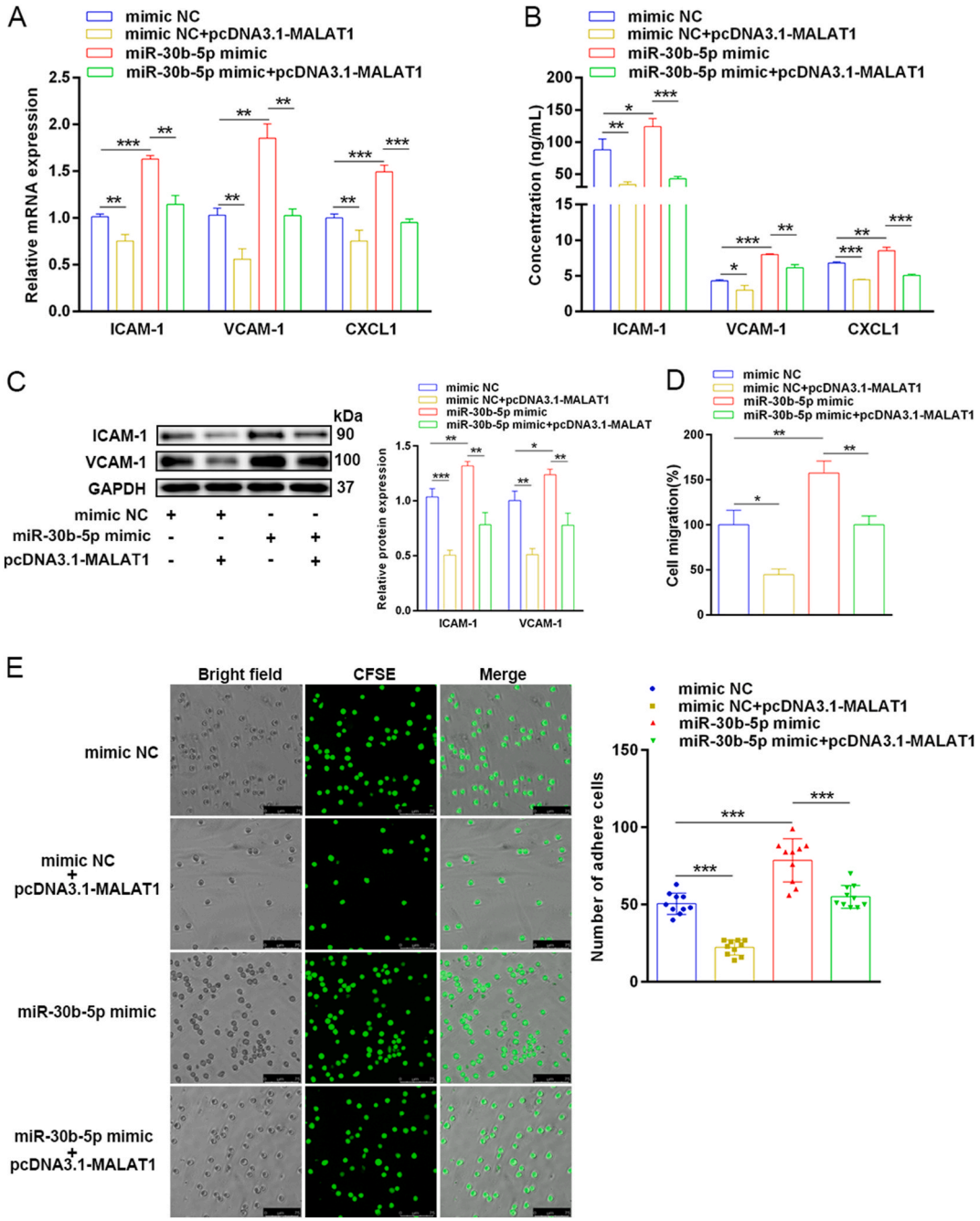

Fig. 5. MALAT1 suppresses the expression of adhesion molecules via miR-30b-5p. (**A**) HUVECs were transfected with miR-30b-5p mimic for 48 h, followed by TNF-α stimulation (10 ng/mL) for 24 h. The mRNA levels of ICAM-1, VCAM-1 and CXCL1 were detected by qRT-PCR, or (**B**) ELISA. (**C**) HUVECs were transfected with miR-30b-5p mimic for 48 h, followed by TNF-α stimulation (10 ng/mL) for 24 h. The protein levels of ICAM-1 and VCAM-1 were detected by Western blot. (**D**) The functional impact of miR-30b-5p and MALAT1 on monocyte migration was assessed by a migration assay. (**E**) The effect of miR-30b-5p and MALAT1 on monocyte-endothelial adhesion was evaluated by an adhesion assay. Scale bar: 75 μm. Data are shown as mean ± standard deviation (n = 3). *, $P < 0.05$; **, $P < 0.01$; ***, $P < 0.001$.

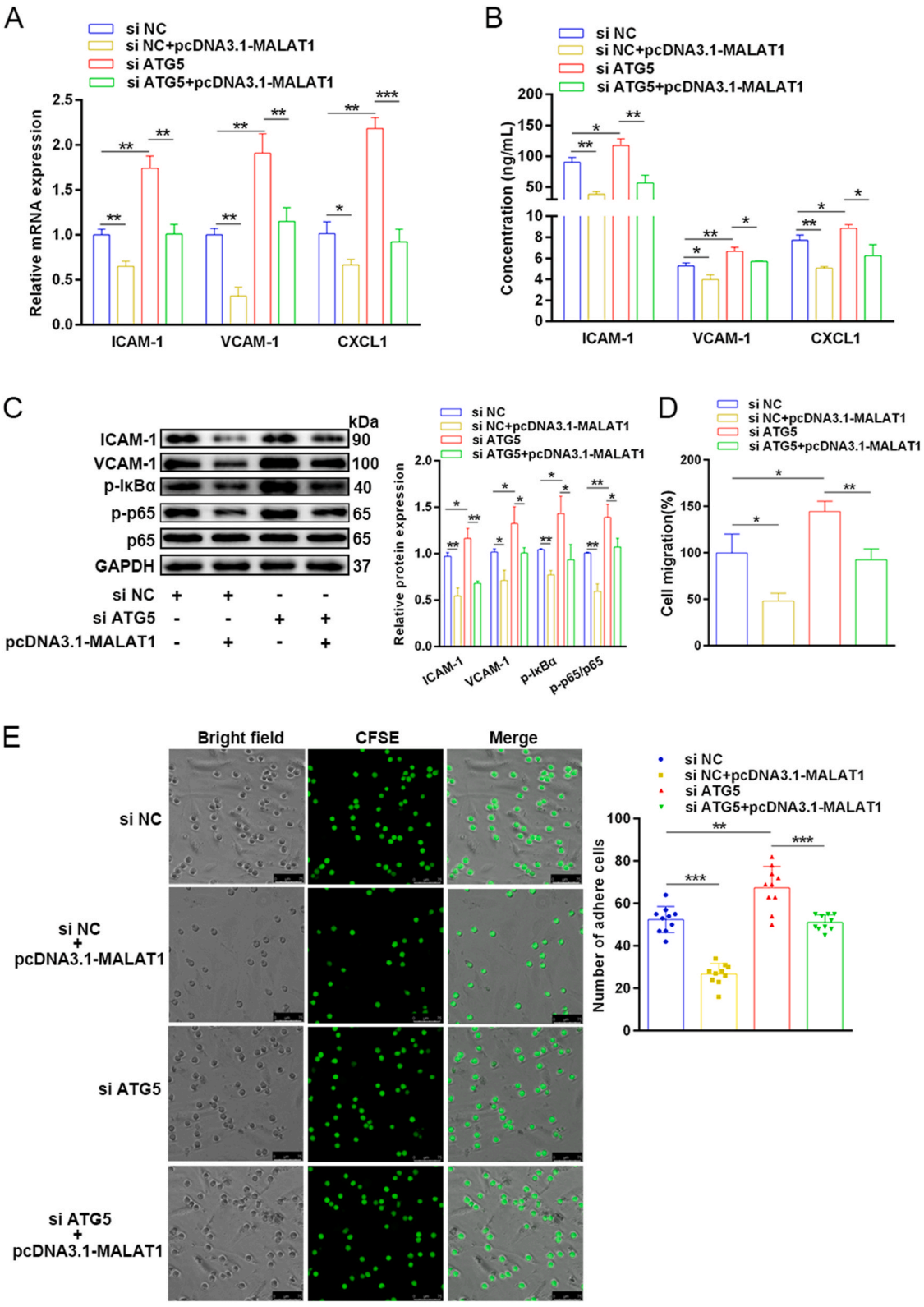

Fig. 6. MALAT1 suppresses the expression of adhesion molecules and monocyte-EC interactions by regulating ATG5. (**A**) HUVECs were transfected with siRNA-ATG5 and/or pcDNA3.1-MALAT1, followed by stimulation with TNF-α (10 ng/mL). The expression levels of ICAM-1, VCAM-1 and CXCL1 were examined by qRT-PCR, and (**B**) ELISA. (**C**) HUVECs were transfected with siRNA-ATG5 and/or pcDNA3.1-MALAT1, followed by

stimulation with TNF-α (10 ng/mL). The expression levels of p-NF-κB, p-IκBα, ICAM-1 and VCAM-1 were quantified by western blotting. (**D**) The effect of ATG5 and MALAT1 expression on monocyte migration was analyzed by a migration assay. (**E**) The effect of ATG5 and MALAT1 on monocyte-EC adhesion was evaluated by a cell adhesion assay. Scale bar: 75 μm. Data are shown as mean ± standard deviation (n = 3). *, $P < 0.05$; **, $P < 0.01$; ***, $P < 0.001$.

We probed whether MALAT1 inhibit NF-κB activity via stimulation of autophagy. HUVECs overexpressing MALAT1 were stimulated with TNF-α, followed by treatment with BafA1. It was observed that inhibition of autophagy reduced the inhibitory effects of MALAT1 on expression of p-NF-κB p65, p-IκBα, ICAM-1, VCAM-1 and CXCL1 (Fig. 3, E-F). Together, these data suggest that MALAT1 suppresses the NF-κB signalling pathway through stimulation of endothelial autophagy.

3.4. MALAT1 acts as a sponge for miR-30b-5p to enhance ATG5 expression in ECs

To further explore the mechanism of endothelial autophagy, we examined the expression of autophagy-related genes, including ATG1, ATG2, ATG3, ATG4A, ATG5, ATG7, ATG10, ATG12, ATG13, and ATG16L, in ECs. We found that MALAT1 overexpression specifically increased the expression of ATG5 (Fig. 4A and B). Next, we sought to elucidate how MALAT1 modulates ATG5 expression. Since MALAT1 has been reported to act as a miRNA sponge, its possible miRNA targets were screened using StarBase v2.0 [19]. Among these MALAT1-specific miRNA candidates, only miR-30b-5p and miR-216b-5p were predicted to bind ATG5 (Fig. 4C). Interestingly, miR-30b-5p and miR-216b-5p have been reported to bind ATG5 and repress autophagy [20,21]. We examined the expression of miR-30b-5p and miR-216b-5p in atherosclerotic aortic tissues and inflamed HUVECs and found that only miR-30b-5p was significantly upregulated (Fig. 4, D-E).

Dual-luciferase reporter and RNA pull-down assays were performed to validate the direct interaction between MALAT1 and miR-30b-5p in ECs (Fig. 4F). Co-transfection of the cells with the miR-30b-5p mimic significantly reduced luciferase activity in cells carrying psicheck2-MALAT1-wt but had no effect on cells carrying psicheck2-MALAT1-mut (Fig. 4, F-G). For the RNA pull-down assay, a biotinylated DNA probe cocktail against MALAT1 was used to enrich endogenous MALAT1. MiR-99a-3p was used as a negative control because it does not form base pairs with MALAT1. MALAT1 specifically enriched miR-30b-5p, rather than miR-99a-3p (Fig. 4H). Furthermore, miR-30b-5p expression reduced in MALAT1 overexpressing HUVECs (Fig. 4I). Next, we determined whether MALAT1 regulates endothelial autophagy by interacting with miR-30b-5p. HUVECs were transfected with miR-30b-5p mimics followed by TNF-α stimulation. ATG5 expression was significantly decreased, and this effect was relieved by MALAT1 overexpression (Fig. 4, J-K). Taken together, these data indicate that MALAT1 binds to miR-30b-5p and enhances ATG5 expression.

3.5. MALAT1 suppresses the expression of cell adhesion molecules via sequestration of miR-30b-5p

We next examined the effects of MALAT1 and miR-30b-5p interaction on monocyte-EC interactions. HUVECs were transfected with miR-30b-5p mimic or NC-mimic and stimulated with TNF-α. It was observed that elevated miR-30b-5p levels increased the expression of ICAM-1, VCAM-1, and CXCL1 compared to the control groups, while overexpression of MALAT1 reduced the robust effect of miR-30b-5p on adhesion molecules (Fig. 5A–C). Functionally, miR-30b-5p enhanced the migration and adhesion of monocytes to ECs, whereas MALAT1 overexpression ameliorated these effects (Fig. 5D and E). Together, these results suggest that MALAT1 suppresses cell adhesion molecules via the sequestration of miR-30b-5p.

3.6. The MALAT1-miR-30b-5p-ATG5 axis suppressed monocyte-EC interaction

To further explore the mechanisms underlying MALAT1 regulation of endothelial adhesion molecule expression, HUVECs were transfected with siRNA-ATG5 and/or pcDNA3.1-MALAT1, followed by TNF-α stimulation. The expression of adhesion molecules was examined using ELISA and qRT-PCR. The results showed that siRNA-mediated suppression of ATG5 expression significantly enhanced the expression of ICAM-1, VCAM-1, and CXCL1, whereas MALAT1 overexpression reduced the expression of ICAM-1, VCAM-1, and CXCL1 (Fig. 6A and B). It was also observed that siRNA-mediated knockdown of ATG5 promoted the expression of p-NF-κB p65, p-IκBα, ICAM-1 and VCAM-1 in inflamed ECs, while MALAT1 overexpression reduced the expression of p-NF-κB p65, p-IκBα, ICAM-1 and VCAM-1 induced by siRNA-ATG5 (Fig. 6C). Additionally, defects in autophagy increased monocyte migration and adhesion to ECs, whereas MALAT1 overexpression alleviated these effects (Fig. 6, D-E). Together, these results suggest that the MALAT1-miR-30b-5p-ATG5 axis suppresses adhesion molecule expression and monocyte-EC interactions.

4. Discussion

In the current study, we discovered that lncRNA MALAT1 suppressed cell adhesion molecule expression and monocyte-EC interactions, thus playing an anti-inflammatory role in vascular endothelial cells. In terms of mechanism, MALAT1 binds miR-30b-5p and stimulates autophagy in ECs. To our knowledge, this is the first study to report that MALAT1 regulates monocyte-EC interactions.

The adhesion of circulating leukocytes such as monocytes to the inflamed endothelium and their transmigration into the subendothelial intima represents a crucial first step in the pathogenesis of atherosclerotic CVD [22]. This is mediated by cell adhesion molecules expressed on the surface of ECs. ICAM-1 is one of the most common adhesion molecules expressed on the surface of ECs and immune cells, and its expression can be elevated by various inflammatory mediators [23]. ICAM-1 is found to be dysregulated in

atherosclerosis-prone aortas. Pretreatment of ApoE$^{-/-}$ mice with anti-ICAM-1 antibody led to an approximately 70% reduction in macrophage homing into atherosclerotic lesions [24]. VCAM-1 is another important adhesion molecule that is induced by inflammatory factors such as TNF-α, LPS, or IL-1β [25]. A study reported that blocking endothelial VCAM-1 with antibodies reduced monocyte adhesion by 75% on early atherosclerotic endothelium [26]. Similarly, we observed that the expression of adhesion molecules and chemokines, i.e. ICAM-1, VCAM-1, P-selectin, CCL2 and CXCL1 was significantly increased in the aortas of ApoE$^{-/-}$ mice and inflamed HUVECs.

With the increase in lncRNA research activity focused on CVD, some lncRNAs have been found to be implicated in atherosclerosis via the regulation of vascular inflammation [27]. MALAT1 is an evolutionarily conserved and abundantly expressed transcript in ECs. Two *in vivo* studies have suggested that a lack of MALAT1 augmented atherosclerotic lesion formation. One study found that MALAT1 was significantly decreased in human plaques compared with normal artery tissues, and exhibited anti-inflammatory properties [17]. Another study observed that MALAT1-deficient ApoE$^{-/-}$ mice developed smaller aortic plaques, and produced higher levels of IFN-γ, TNF-α and IL-6 [28]. However, some controversial findings have also been reported. A study showed that MALAT1 played a proinflammatory role in ECs through regulating the miR-590/STAT3 axis [29]. Another studied found that MALAT1 induced inflammasome activation and reactive oxygen species (ROS) production in mouse (*in vivo*) and microglial cell (*in vitro*) models [30]. We speculate that these inconsistent findings may be explained by factors such as differences in cell types, stimuli involved and methodology adopted. In the present study, we found that the expression of MALAT1 was reduced in both the aortas of ApoE$^{-/-}$ mice and inflamed ECs, and overexpression of MALAT1 suppressed the expression of adhesion molecules and monocyte-EC interactions. Thus, our data support MALAT1 playing an anti-inflammatory role in ECs. However, we did not identify which adhesion molecule, ICAM-1 or VCAM-1, exerts a crucial role in this process.

Cell adhesion molecules are known as established inflammatory biomarkers of atherosclerosis that are regulated through NF-κB signalling [4]. Our data show that MALAT1 suppressed the expression of p-p65 and p-IκBα, and decreased the number of nuclei containing p65, thus suggesting that MALAT1 interferes with NF-κB activity. Autophagy and inflammation are known to interact on multiple levels. Our previous study had found that stimulation of endothelial autophagy reduced the expression of cell adhesion molecules through inhibiting NF-κB activity. In addition, MALAT1 has been reported to enhance autophagy in various cells including ECs [31,32]. In the present study, we observed that MALAT1 overexpression significantly stimulated autophagy in ECs, and suppression of autophagy by inhibitors abolished its effect on NF-κB and adhesion molecules. ATG5 is a key gene in the autophagy process, and a recent study has reported that MALAT1 regulates autophagy-related chemoresistance via ATG5 in gastric cancer [33]. We found that MALAT1 overexpression specifically increased ATG5, and knockdown of ATG5 significantly alleviated the regulatory effect of MALAT1 on NF-κB activity and cell adhesion molecule expression. Our data suggest that MALAT1 plays an anti-inflammatory role via enhancing ATG5-mediated autophagy in ECs.

Some studies have reported that MALAT1 binds and sequesters miRNAs and competitively represses miRNA functions [34]. Considering the enhancement effect of MALAT1 on ATG5 in our study, we speculated that MALAT1 might upregulate ATG5 by binding to miRNAs. Bioinformatics analysis revealed that miR-30b-5p could bind to both MALAT1 and ATG5, and these putative interactions were confirmed by luciferase reporter and pull-down assays. MiR-30b-5p overexpression strengthened cell adhesion molecule expression and reduced ATG5 expression, while MALAT1 overexpression alleviated the robustly positive effect of miR-30b-5p on endothelial autophagy, and subsequently repressed adhesion molecule expression and monocyte-EC interactions. Thus, our data suggest that MALAT1 suppresses ATG5, and that this depends at least in part on binding to miR-30b-5p. A previous study has found that inhibition of the miR-30 family contributes to endoplasmic reticulum stress in vascular smooth muscle cells [35]. *In vivo* experiments involving the use of heart-specific miR-30b expressing transgenic mice showed reduced necrosis and myocardial infarction size during ischemia/reperfusion injury [36]. These studies suggest that miR-30b-5p may be an important regulator of CVD, and this is also supported by our data. Notably, MALAT1 is known to bind to other miRNAs that induce cell autophagy, such as miR-423-5p [37], and may also affect gene expression by epigenetic mechanisms or by interfering with proinflammatory transcription factors.

The present study has some limitations. First, human samples were lacking to examine the association between MALAT1 and cell adhesion molecules in atherosclerotic lesions. Second, although we demonstrated that MALAT1 interacts with miR-30b-5p to mediate autophagy and suppress monocyte-EC binding, we did not exclude other miRNAs from participating in this process. Third, *in vivo* evidence is needed to affirm these findings.

5. Conclusions

The present study demonstrates that MALAT1 plays an anti-atherosclerosis role by suppressing cell adhesion molecule expression and monocyte-EC interactions. MALAT1 exerts this effect by depending at least in part on binding and sequestering miR-30b-5p and competitively interfering with its role in endothelial autophagy. The findings of this study suggest an important role of MALAT1 at the early stage of atherosclerosis.

Ethical approval

The animal experiments were conducted following protocols approved by the Laboratory Animal Ethics Committee of Meizhou People's Hospital (NO: GDY2002177) and complied with the national guidelines for the care and use of animals.

Funding

This research was supported by the National Natural Science Foundation for Young Scientists of China (82000410); Guangdong Natural Science Foundation (2022A1515011860, 2022A1515012590); Medical Research Foundation of Guangdong Province (A2023324); Scientific Research and Cultivation Project of Meizhou People's Hospital (PY–C2022017).

Data availability statement

The data used is available in the supplementary material and upon reasonable request.

Consent for publication

Not applicable.

CRediT authorship contribution statement

Xiaodong Gu: Writing – original draft. **Jingyuan Hou:** Writing – review & editing. **Jiawei Rao:** Data curation. **Ruiqiang Weng:** Investigation. **Sudong Liu:** Writing – review & editing, Project administration.

Declaration of competing interest

The authors declare that they have no known competing financial interestsor personal relationships that could have appeared to influence the work reported in this paper.

Acknowledgements

Not applicable.

Appendix A. Supplementary data

Supplementary data to this article can be found online at https://doi.org/10.1016/j.heliyon.2024.e28882.

References

[1] S.M. Manemann, et al., Recent trends in cardiovascular disease deaths: a state specific perspective, BMC Publ. Health 21 (1) (2021) 1031.
[2] J.L.M. Björkegren, A.J. Lusis, Atherosclerosis: recent developments, Cell 185 (10) (2022) 1630–1645.
[3] I. Mitroulis, et al., Leukocyte integrins: role in leukocyte recruitment and as therapeutic targets in inflammatory disease, Pharmacol. Ther. 147 (2015) 123–135.
[4] M. Yin, et al., Cell adhesion molecule-mediated therapeutic strategies in atherosclerosis: from a biological basis and molecular mechanism to drug delivery nanosystems, Biochem. Pharmacol. 186 (2021) 114471.
[5] N.T. Mulvihill, et al., Prediction of cardiovascular risk using soluble cell adhesion molecules, Eur. Heart J. 23 (20) (2002) 1569–1574.
[6] C. Sturtzel, Endothelial cells, Adv. Exp. Med. Biol. 1003 (2017) 71–91.
[7] J.K. DiStefano, G.S. Gerhard, Long noncoding RNAs and human liver disease, Annu. Rev. Pathol. 17 (2022) 1–21.
[8] A.B. Herman, D. Tsitsipatis, M. Gorospe, Integrated lncRNA function upon genomic and epigenomic regulation, Mol. Cell 82 (12) (2022) 2252–2266.
[9] J.D. Ransohoff, Y. Wei, P.A. Khavari, The functions and unique features of long intergenic non-coding RNA, Nat. Rev. Mol. Cell Biol. 19 (3) (2018) 143–157.
[10] A. Kohlmaier, L.M. Holdt, D. Teupser, Long noncoding RNAs in cardiovascular disease, Curr. Opin. Cardiol. 38 (3) (2023) 179–192.
[11] F. Fasolo, et al., Long noncoding RNA MIAT controls advanced atherosclerotic lesion formation and plaque destabilization, Circulation 144 (19) (2021) 1567–1583.
[12] L.M. Holdt, et al., Alu elements in ANRIL non-coding RNA at chromosome 9p21 modulate atherogenic cell functions through trans-regulation of gene networks, PLoS Genet. 9 (7) (2013) e1003588.
[13] P. Han, et al., A long noncoding RNA protects the heart from pathological hypertrophy, Nature 514 (7520) (2014) 102–106.
[14] P. Ji, et al., MALAT-1, a novel noncoding RNA, and thymosin beta4 predict metastasis and survival in early-stage non-small cell lung cancer, Oncogene 22 (39) (2003) 8031–8041.
[15] K.M. Michalik, et al., Long noncoding RNA MALAT1 regulates endothelial cell function and vessel growth, Circ. Res. 114 (9) (2014) 1389–1397.
[16] M. Brock, et al., Analysis of hypoxia-induced noncoding RNAs reveals metastasis-associated lung adenocarcinoma transcript 1 as an important regulator of vascular smooth muscle cell proliferation, Exp. Biol. Med. 242 (5) (2017) 487–496.
[17] S. Cremer, et al., Hematopoietic deficiency of the long noncoding RNA MALAT1 promotes atherosclerosis and plaque inflammation, Circulation 139 (10) (2019) 1320–1334.
[18] X. Gu, et al., Endothelial miR-199a-3p regulating cell adhesion molecules by targeting mTOR signaling during inflammation, Eur. J. Pharmacol. 925 (2022) 174984.
[19] J.H. Li, et al., starBase v2.0: decoding miRNA-ceRNA, miRNA-ncRNA and protein-RNA interaction networks from large-scale CLIP-Seq data, Nucleic Acids Res. 42 (Database issue) (2014) D92–D97.
[20] N. Zhang, et al., PAX5-induced upregulation of IDH1-AS1 promotes tumor growth in prostate cancer by regulating ATG5-mediated autophagy, Cell Death Dis. 10 (10) (2019) 734.
[21] Z. Liu, et al., Long non-coding RNA HNF1A-AS1 functioned as an oncogene and autophagy promoter in hepatocellular carcinoma through sponging hsa-miR-30b-5p, Biochem. Biophys. Res. Commun. 473 (4) (2016) 1268–1275.
[22] J.L.M. Bjorkegren, A.J. Lusis, Atherosclerosis: recent developments, Cell 185 (10) (2022) 1630–1645.

[23] T.M. Bui, H.L. Wiesolek, R. Sumagin, ICAM-1: a master regulator of cellular responses in inflammation, injury resolution, and tumorigenesis, J. Leukoc. Biol. 108 (3) (2020) 787–799.
[24] S.S. Patel, et al., Inhibition of alpha4 integrin and ICAM-1 markedly attenuate macrophage homing to atherosclerotic plaques in ApoE-deficient mice, Circulation 97 (1) (1998) 75–81.
[25] M.F. Troncoso, et al., VCAM-1 as a predictor biomarker in cardiovascular disease, Biochim. Biophys. Acta, Mol. Basis Dis. 1867 (9) (2021) 166170.
[26] Y. Huo, A. Hafezi-Moghadam, K. Ley, Role of vascular cell adhesion molecule-1 and fibronectin connecting segment-1 in monocyte rolling and adhesion on early atherosclerotic lesions, Circ. Res. 87 (2) (2000) 153–159.
[27] T. Josefs, R.A. Boon, The long non-coding road to atherosclerosis, Curr. Atherosclerosis Rep. 22 (10) (2020) 55.
[28] M. Gast, et al., Immune system-mediated atherosclerosis caused by deficiency of long non-coding RNA MALAT1 in ApoE-/-mice, Cardiovasc. Res. 115 (2) (2019) 302–314.
[29] Q. Zhou, et al., LncRNA MALAT1 promotes STAT3-mediated endothelial inflammation by counteracting the function of miR-590, Cytogenet. Genome Res. 160 (10) (2020) 565–578.
[30] L.J. Cai, et al., LncRNA MALAT1 facilitates inflammasome activation via epigenetic suppression of Nrf2 in Parkinson's disease, Mol. Brain 13 (1) (2020) 130.
[31] J. Yang, et al., LncRNA MALAT1 enhances ox-LDL-induced autophagy through the SIRT1/MAPK/NF-κB pathway in macrophages, Curr. Vasc. Pharmacol. 18 (6) (2020) 652–662.
[32] K. Wang, et al., Ox-LDL-induced lncRNA MALAT1 promotes autophagy in human umbilical vein endothelial cells by sponging miR-216a-5p and regulating Beclin-1 expression, Eur. J. Pharmacol. 858 (2019) 172338.
[33] Y.F. Zhang, et al., Propofol facilitates cisplatin sensitivity via lncRNA MALAT1/miR-30e/ATG5 axis through suppressing autophagy in gastric cancer, Life Sci. 244 (2020) 117280.
[34] R. Sun, L. Zhang, Long non-coding RNA MALAT1 regulates cardiomyocytes apoptosis after hypoxia/reperfusion injury via modulating miR-200a-3p/PDCD4 axis, Biomed. Pharmacother. 111 (2019) 1036–1045.
[35] M. Chen, et al., Downregulation of the miR-30 family microRNAs contributes to endoplasmic reticulum stress in cardiac muscle and vascular smooth muscle cells, Int. J. Cardiol. 173 (1) (2014) 65–73.
[36] K. Wang, et al., E2F1-regulated miR-30b suppresses Cyclophilin D and protects heart from ischemia/reperfusion injury and necrotic cell death, Cell Death Differ. 22 (5) (2015) 743–754.
[37] C. Ferri, et al., MiR-423-5p prevents MALAT1-mediated proliferation and metastasis in prostate cancer, J. Exp. Clin. Cancer Res. 41 (1) (2022) 20.